JOURNAL OF GUIDANCE, CONTROL, AND DYNAMICS
Vol. 31, No. 4, July–August 2008

Engineering Notes

ENGINEERING NOTES are short manuscripts describing new developments or important results of a preliminary nature. These Notes should not exceed 2500 words (where a figure or table counts as 200 words). Following informal review by the Editors, they may be published within a few months of the date of receipt. Style requirements are the same as for regular contributions (see inside back cover).

Simple Real-Time Stabilization of Vertical Takeoff and Landing Aircraft with Bounded Signals

A. Sanchez*
Universitè de Technologie de Compiègne, 60205 Compiègne, France
P. Garcia†
Technical University of Valencia, E-46022 Valencia, Spain
and
P. Castillo‡ and R. Lozano§
Universitè de Technologie de Compiègne, 60205 Compiègne, France

DOI: 10.2514/1.32157

Nomenclature

$C(\eta, \dot{\eta})$	=	Coriolis matrix
E_z	=	unitary vector in the z coordinate
$F_\xi \in \mathbb{R}^3$	=	translational forces applied to the rotorcraft
f	=	vector of the principal nonconservative forces applied to the object, including thrusts and drag terms associated with the rotors
f_i	=	force produced by motor i
g	=	acceleration due to gravity
$\mathbf{I} \in \mathbb{R}^{3\times3}$	=	inertia matrix around the center of mass (expressed in the body fixed frame)
$\mathbb{J}(\eta)$	=	inertia matrix for the full rotational kinetic energy of the helicopter expressed directly in terms of the generalized coordinates η
m	=	mass of the rigid object
$\dot{\eta}$	=	generalized velocities in the region in which the Euler angles are valid
$q = (\xi\eta)^T$	=	vector of the generalized coordinates of the aircraft
$R(\psi, \theta, \phi) \in SO(3)$	=	rotational matrix
T_{rot}	=	rotational kinetic energy
T_{trans}	=	translational kinetic energy
U	=	potential energy of the rigid object
u_i	=	control input i
v	=	linear velocity expressed in the inertial frame
$\eta = (\psi, \theta, \phi)^T$	=	orientation of the rotorcraft representing the Euler angles (yaw, pitch, and roll angles)
$\xi = (x, y, z)^T$	=	position of the center of mass of the aircraft relative to a fixed origin; x and y are coordinates in the horizontal plane, and z is the vertical position
$\tau = (\tau_\psi, \tau_\theta, \tau_\phi)^T$	=	yawing, pitching, and rolling moments, respectively
Ω	=	angular velocity of the airframe expressed in the body fixed frame
$\hat{\Omega}$	=	skew-symmetric matrix of the vector Ω
ω	=	angular velocity vector expressed in the body fixed frame

I. Introduction

UNMANNED aerial vehicles (UAVs) have been referred to in many ways; remotely piloted vehicles (RPV), drones, robot planes, and pilotless aircraft are a few such names. Most often called UAVs, they are defined by the U.S. Department of Defense as powered, aerial vehicles that do not carry a human operator, use aerodynamic forces to provide vehicle lift, can fly autonomously or be piloted remotely, can be expendable or recoverable, and can carry a payload. UAVs differ from RPVs in that some UAVs can fly autonomously. UAVs are either described as single air vehicles (with associated surveillance sensors) or a UAV system, which usually consists of three to six air vehicles, a ground control station, and support equipment. There are a number of reasons why UAVs have only recently been given a higher priority. Technology is now available that was not available just a few short years ago. UAVs have traditionally been used for reconnaissance and surveillance, but today they are being employed in roles and applications that their designers never envisioned. The unanticipated flexibility and capability of UAVs has led some analysts to suggest that more, if not most, of the missions currently undertaken by manned aircraft could be turned over to unmanned aerial platforms and that manned and unmanned aircraft could operate together. UAVs range from the size of an insect to a commercial aircraft.More recently, a growing interest in unmanned aerial vehicles has been shown among the research community [1–5]. Being able to design an unmanned vertical takeoff and landing (VTOL) vehicle that is highly maneuverable and extremely stable is an important contribution to the field of aerial robotics because potential applications are tremendous. In practical applications, the position in space of the VTOL unmanned aerial vehicle is generally controlled by an operator through a remote control system using a visual feedback from an onboard camera, whereas the attitude is automatically stabilized via an onboard controller. The attitude controller is an important feature because it allows the vehicle to maintain a desired horizontal orientation and, hence, prevents the vehicle from flipping over and crashing when the pilot performs the desired maneuvers [6,7]. Most of the existing attitude controllers in the literature are based on the use of the quaternion representation to describe the attitude of the body [8,9].

In this paper we present a new control algorithm for a VTOL aircraft whose convergence analysis is relatively simple compared

Received 15 May 2007; revision received 20 December 2007; accepted for publication 20 December 2007.

*CNRS, Heudiasyc. B.P. 20529; asanchez@hds.utc.fr.
†Department of Systems Engineering and Control, pggil@isa.upv.es.
‡CNRS, Heudiasyc. B.P. 20529; castillo@hds.utc.fr.
§CNRS, Heudiasyc. B.P. 20529; rlozano@hds.utc.fr.

with other controllers proposed in the literature. We present a new approach based on Lyapunov analysis and saturation functions to control a VTOL aircraft, which can lead to further developments in nonlinear systems. The controller has not only been tested in numerical simulations, but also in a real-time application. We applied it to control the altitude of a radio-controlled electrical quad-rotor helicopter and to stabilize the quad-rotor helicopter in free flight. The simplicity of the algorithm was very useful in the practical application and, in particular, it simplified the tuning of the controller parameters.

This paper is organized as follows. In Sec. II, the system dynamics of a VTOL aircraft are presented. Section III is devoted to establishing the control strategy. In Sec. IV, we compare the performance of the proposed controller with respect to others using nested saturations. The experimental results are shown in Sec. V, and the conclusions are given in Sec. VI.

II. Problem Statement

The mathematical model to describe the dynamics of a VTOL aircraft assuming small angles around a given position can be obtained by representing the aircraft as a solid body evolving in a three-dimensional space and subject to the thrusts and torques and using two classical methods, the Euler–Lagrange approach and the Newton–Euler approach.

The Newton–Euler formalism is given by (see [10,11])

$$\dot{\xi} = v, \qquad \dot{R} = R, \qquad m\dot{v} = f, \qquad \mathbf{I}\dot{\Omega} = -\Omega \times \mathbf{I}\Omega + \tau \quad (1)$$

and the Euler–Lagrange approach using the Lagrangian is defined as $L(q, \dot{q}) = T_{\text{trans}} + T_{\text{rot}} - U$, where $T_{\text{trans}} = \frac{m}{2}\dot{\xi}^T\dot{\xi}$, $T_{\text{rot}} = \frac{1}{2}\Omega^T\mathbf{I}\Omega$, and $U = mgz$.

Some examples of VTOL aircraft are the well-known planar vertical takeoff and landing (PVTOL) aircraft (see Fig. 1) and the quad-rotor aircraft (see Fig. 2).

1) PVTOL Aircraft: The PVTOL aircraft is a mathematical model of a flying object that evolves in a vertical plane [1]. This aircraft has 3 degrees of freedom, (x, z, ϕ), corresponding to its position in the x coordinate, the altitude, and the roll angle. The PVTOL aircraft has two independent thrusters that produce a force and a moment and, thus, it is underactuated because it has 3 degrees of freedom and only two inputs.

From Fig. 1 and using the Newton–Euler approach, we can obtain the basic equations of motion for the PVTOL aircraft given by (see [4])

$$\begin{aligned} m\ddot{x} &= -u\sin\phi + \varepsilon\tau_\phi\cos\phi, \qquad I\ddot{\phi} = \tau_\phi, \\ m\ddot{z} &= u\cos\phi + \varepsilon\tau_\phi\sin\phi - mg \end{aligned} \quad (2)$$

The control inputs $u = f_1 + f_2$ and τ_ϕ are the thrust (directed out of the bottom of the aircraft) and the rolling moment. The parameter ε is a small coefficient that characterizes the coupling between the rolling moment and the lateral acceleration of the aircraft. This coefficient ε is very small ($\varepsilon \ll 1$), not always well known, and also neglected. Thus, neglecting ε, the simplified model is

$$m\ddot{x} = -u\sin\phi, \qquad I\ddot{\phi} = \tau_\phi, \qquad m\ddot{z} = u\cos\phi - mg \quad (3)$$

Furthermore, Olfati-Saber [12] has shown that, by an appropriate change of coordinates, we can transform the system (2) into an equivalent system of the same form, (3), but with $\varepsilon \neq 0$.

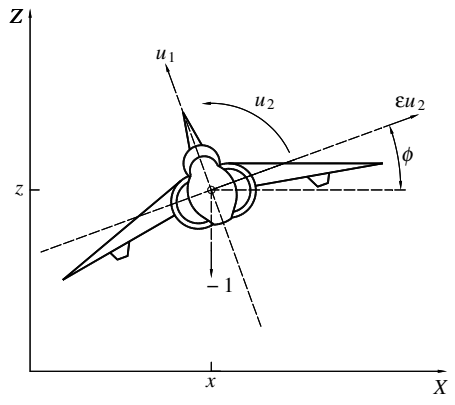

Fig. 1 The PVTOL aircraft.

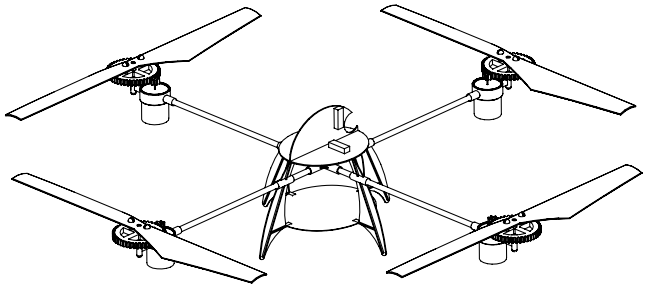

Fig. 2 The quad-rotor aircraft.

2) Quad-Rotor Helicopter: The quad-rotor helicopter has four rotors and is mechanically simpler and easier to repair than a classical helicopter. The quad-rotor control problem is similar to that of controlling two PVTOL aircraft. The quad-rotor helicopter has some similarities with the PVTOL aircraft. Indeed, if the roll (or pitch) and yaw angles are set to zero, the quad-rotor reduces to a PVTOL aircraft and can be viewed as two PVTOL aircraft connected such that their axes are orthogonal. The quad-rotor or the PVTOL aircraft are useful prototypes for learning about aerodynamic phenomena in flying machines that can hover.

Using the Euler–Lagrange approach, we obtain

$$m\ddot{\xi} + mgzE_z = F_\xi, \qquad \mathbb{J}\ddot{\eta} + C(\eta, \dot{\eta})\dot{\eta} = \tau \quad (4)$$

The approximated mathematical model that describes the dynamics of a quad-rotor aircraft assuming small angles is

$$\begin{aligned} \ddot{x} &= u(\sin\phi\sin\psi + \cos\phi\cos\psi\sin\theta), \qquad \ddot{\psi} = \tau_\psi, \\ \ddot{y} &= -u(\cos\psi\sin\phi - \cos\phi\sin\theta\sin\psi), \qquad \ddot{\theta} = \tau_\theta, \\ \ddot{z} &= u\cos\theta\cos\phi - g, \qquad \ddot{\phi} = \tau_\phi \end{aligned} \quad (5)$$

Note that systems (3) and (5) have a lot of similarities. First, in both systems the attitude is given by two integrators in cascade, that is, $\ddot{\eta} = \tau_\eta$. Note also that this equation also represents the dynamic of a quad-rotor aircraft mounted on a 3-DOF pivot joint such that the body can freely roll, pitch, and yaw.¶ Second, when the altitude and the yaw angle is stabilized in both systems, their remaining subsystems are very similar [note the dynamics for x and ϕ in Eq. (3) and y and ϕ in Eq. (5)].

III. Control Strategy

In this section a simple nonlinear control strategy to stabilize a quad-rotor aircraft using saturation functions is proposed. The control law is such that, when the system is in the linear part of the saturation function, it can be seen as a linear controller. It is well known [1] that a conventional linear control (proportional integral derivative or proportional derivative) can stabilize a VTOL aircraft in special conditions, that is, without significant disturbances. In this paper, it is shown that by using saturation functions in the control law the performance of the closed-loop system in real conditions are improved. This fact is shown with experimental results. The main goal in this paper is to show a simple proof of stability of the closed-loop system using saturation functions and the application of the controller in real-time experiments.

¶Data available online at Quanser, 3 DOF Hover, http://www.quanser.com/english/downloads/products/3DOF_Hover.pdf [retrieved 30 April 2008].

First, we present in this section our study of controlling a chain of integrators in cascade. After that, we will validate the proposed control strategy to stabilize the quad-rotor aircraft. Note that the control law proposed is obtained using a sequential approach based on Lyapunov theory.

A. Two Integrators in Cascade

Let us consider the system

$$\dot{x}_1 = \beta x_2, \qquad \dot{x}_2 = u \tag{6}$$

where $\beta \neq 0$ is a constant. Propose the following control input

$$u = -\sigma_{b_2}(\bar{k}_2 x_2) - \sigma_{b_1}(\bar{k}_1 x_1) \tag{7}$$

where $\sigma_{b_i}(\cdot)$ is a saturation function (see Fig. 3) and $b_i, \bar{k}_i > 0$, $i = 1, 2$, are constant.

Define the following positive function:

$$V_1 = \tfrac{1}{2}x_2^2 \tag{8}$$

This yields

$$\dot{V}_1 = x_2\dot{x}_2 = -x_2[\sigma_{b_2}(\bar{k}_2 x_2) + \sigma_{b_1}(\bar{k}_1 x_1)] \tag{9}$$

Note that if $|\bar{k}_2 x_2| > b_1$ then $\dot{V}_1 < 0$. This implies that $\exists T_1$ such that $|x_2(t)| \leq b_1/\bar{k}_2 \ \forall\, t > T_1$. Choosing $b_2 > b_1$, this yields

$$u = -\bar{k}_2 x_2 - \sigma_{b_1}(\bar{k}_1 x_1) \qquad \forall\ t > T_1 \tag{10}$$

Define

$$\nu = \frac{\bar{k}_2}{\beta}x_1 + x_2 \tag{11}$$

differentiating Eq. (11) and using (10) yields

$$\dot{\nu} = \frac{\bar{k}_2}{\beta}\dot{x}_1 + \dot{x}_2 = \bar{k}_2 x_2 + u = -\sigma_{b_1}[(\bar{k}_1/\bar{k}_2)(\beta\nu - \beta x_2)] \qquad \forall\ t > T_1 \tag{12}$$

Define

$$V_2 = \tfrac{1}{2}\nu^2 \tag{13}$$

This yields

$$\dot{V}_2 = \nu\dot{\nu} = -\nu\sigma_{b_1}[(\bar{k}_1/\bar{k}_2)(\beta\nu - \beta x_2)]$$

Note that, if $|\nu| > b_1/\bar{k}_2$, then $\dot{V}_2 < 0$. This implies that $\exists T_2 > T_1$ such that

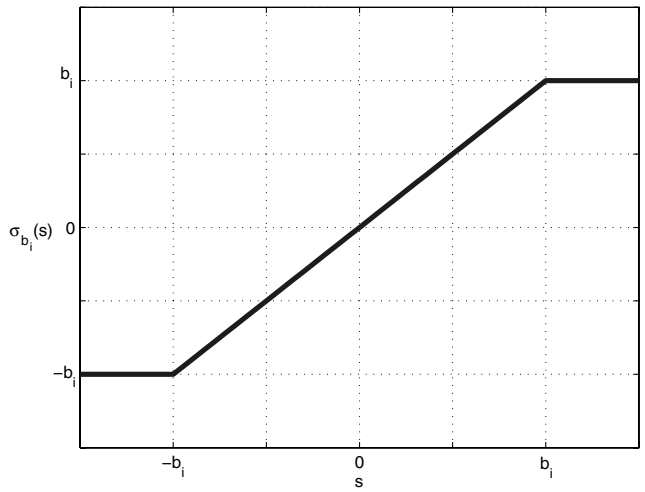

Fig. 3 Ramp-shaped saturation function.

$$|\nu| \leq b_1/\bar{k}_2 \tag{14}$$

If

$$\bar{k}_2^2 \geq 2\bar{k}_1|\beta| \tag{15}$$

then $(\bar{k}_1/\bar{k}_2)|\beta\nu - \beta x_2| \leq b_1$.

Thus, from Eqs. (10), (14), and (15), we obtain for $t > T_2$

$$u = -\bar{k}_1 x_1 - \bar{k}_2 x_2 = -K^T\bar{x} \tag{16}$$

where

$$K = \begin{pmatrix} \bar{k}_1 \\ \bar{k}_2 \end{pmatrix} \quad \text{and} \quad \bar{x} = \begin{pmatrix} x_1 \\ x_2 \end{pmatrix}$$

Rewriting system (6), we have

$$\dot{\bar{x}} = A\bar{x} + Bu \tag{17}$$

where

$$A = \begin{pmatrix} 0 & \beta \\ 0 & 0 \end{pmatrix}, \qquad B = \begin{pmatrix} 0 \\ k \end{pmatrix}$$

Using Eq. (16), we have

$$\dot{\bar{x}} = (A - BK^T)\bar{x} \tag{18}$$

Then, we need to choose $\bar{k}_1$ and $\bar{k}_2$ such that the matrix $(A - BK^T)$ is stable and Eq. (15) is valid.

B. Four Integrators in Cascade

Let us consider the following system:

$$\dot{x}_1 = \alpha x_2, \qquad \dot{x}_3 = \gamma x_4, \qquad \dot{x}_2 = \beta x_3, \qquad \dot{x}_4 = u \tag{19}$$

where α, β, and $\gamma \neq 0$ are constant. Proposing

$$u = -\sigma_{b_4}(k_4 z_4) - \xi_1 \tag{20}$$

where $z_4 = x_4$, $|\sigma_{b_i}| < b_i$ is a saturation function, $|\xi_i| \leq b_{\xi_i}$ will be defined later to ensure asymptotically stability, and b_i, b_{ξ_i}, and $k_i > 0$ are constant. Proposing the following positive function:

$$\bar{V}_1 = \tfrac{1}{2}z_4^2 \tag{21}$$

This yields

$$\dot{\bar{V}}_1 = z_4\dot{z}_4 = -z_4(\sigma_{b_4}(k_4 z_4) + \xi_1) \tag{22}$$

Note that if $|k_4 z_4| > b_{\xi_1}$ then $\dot{\bar{V}}_1 < 0$. This implies that $\exists T_1$ such that $|k_4 z_4(t)| \leq b_{\xi_1}\ \forall\, t > T_1$. Choosing $b_4 > b_{\xi_1}$, we have

$$u = -k_4 z_4 - \xi_1 \quad \forall\ t > T_1 \tag{23}$$

Define

$$z_3 = \frac{k_4}{\gamma}x_3 + z_4 \tag{24}$$

Differentiating Eq. (24) and using (23)

$$\dot{z}_3 = \frac{k_4}{\gamma}\dot{x}_3 + \dot{z}_4 = k_4 z_4 + u = -\xi_1 \quad \forall\ t > T_1 \tag{25}$$

Define

$$\xi_1 = \sigma_{b_3}(k_3 z_3) + \xi_2 \tag{26}$$

thus, $|\xi_1| \leq b_{\xi_1} = b_3 + b_{\xi_2}$. Proposing

$$\bar{V}_2 = \frac{1}{2} z_3^2 \tag{27}$$

this yields

$$\dot{\bar{V}}_2 = z_3 \dot{z}_3 = -z_3(\sigma_{b_3}(k_3 z_3) + \xi_2) \tag{28}$$

If $|k_3 z_3| > b_{\xi_2}$ then $\dot{\bar{V}}_2 \leq 0$. This implies that $\exists T_2$ such that $|k_3 z_3(t)| \leq b_{\xi_2}\ \forall\ t > T_2$. Choosing $b_3 > b_{\xi_2}$, we have

$$\dot{z}_3 = -k_3 z_3 - \xi_2 \quad \forall\ t > T_2 \tag{29}$$

Define

$$z_2 = z_3 + \frac{k_3 k_4}{\beta\gamma} x_2 + \frac{k_3}{\gamma} x_3 \tag{30}$$

Differentiating Eq. (30), we obtain

$$\dot{z}_2 = \dot{z}_3 + \frac{k_3 k_4}{\beta\gamma} \dot{x}_2 + \frac{k_3}{\gamma} \dot{x}_3 = -\xi_2 \tag{31}$$

Define

$$\xi_2 = \sigma_{b_2}(k_2 z_2) + \xi_3 \tag{32}$$

where $|\xi_2| \leq b_{\xi_2} = b_2 + b_{\xi_3}$. Proposing the following definite function

$$\bar{V}_3 = \tfrac{1}{2} z_2^2 \tag{33}$$

yields

$$\dot{\bar{V}}_3 = z_2 \dot{z}_2 = -z_2(\sigma_{b_2}(k_2 z_2) + \xi_3) \tag{34}$$

If $|k_2 z_2| \leq b_{\xi_3}$ then $\dot{\bar{V}}_3 \leq 0$, which implies that $\exists T_3$ such that $|k_2 z_2(t)| \leq b_{\xi_3}\ \forall\ t > T_3$. Choosing $b_2 > b_{\xi_3}$, we have

Table 1 Gain values used in the control laws (41) and (47–49)

	Controller (41) and (47)	Controller (48) and (49)
Altitude	$a_1 = 0.5$ $a_2 = 0.1$ $n_1 = 0.5$ $n_2 = 0.25$ $n_3 = 1.2$	$\bar{a}_1 = 0.5$ $\bar{a}_2 = 0.1$ $p = 1.2$
(x, ϕ) subsystem	$k_1 = 1$ $k_2 = 0.1$ $k_3 = 1$ $k_4 = 1$ $b_1 = 0.06$ $b_2 = 0.1$ $b_3 = 0.17$ $b_4 = 0.193$	$a = 0.523$ $b = 0.261$ $c = 0.13$ $d = 0.06$

$$\dot{z}_2 = -k_2 z_2 - \xi_3$$

Define

$$z_1 = z_2 + \frac{k_2 k_3 k_4}{\beta\gamma\alpha} x_1 + \frac{k_2}{\gamma} x_3 + \frac{k_2(k_3 + k_4)}{\beta\gamma} x_2 \tag{35}$$

Differentiating Eq. (35) yields

$$\dot{z}_1 = -\xi_3 \tag{36}$$

Define

$$\xi_3 = \sigma_{b_1}(k_1 z_1) \tag{37}$$

where $b_{\xi_3} = b_1$. Proposing the following definite function

$$\bar{V}_4 = \tfrac{1}{2} z_1^2 \tag{38}$$

yields

$$\dot{\bar{V}}_4 = z_1 \dot{z}_1 = -z_1 \sigma_{b_1}(k_1 z_1) \tag{39}$$

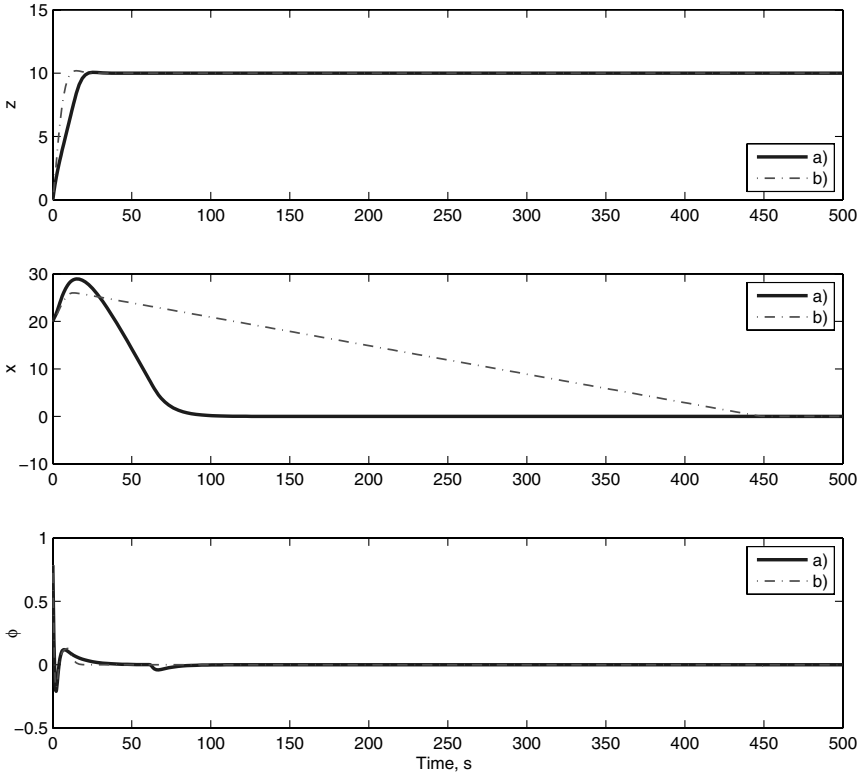

Fig. 4 States z, x, and ϕ of the system: a) controllers (41) and (47), and b) controllers (48) and (49).

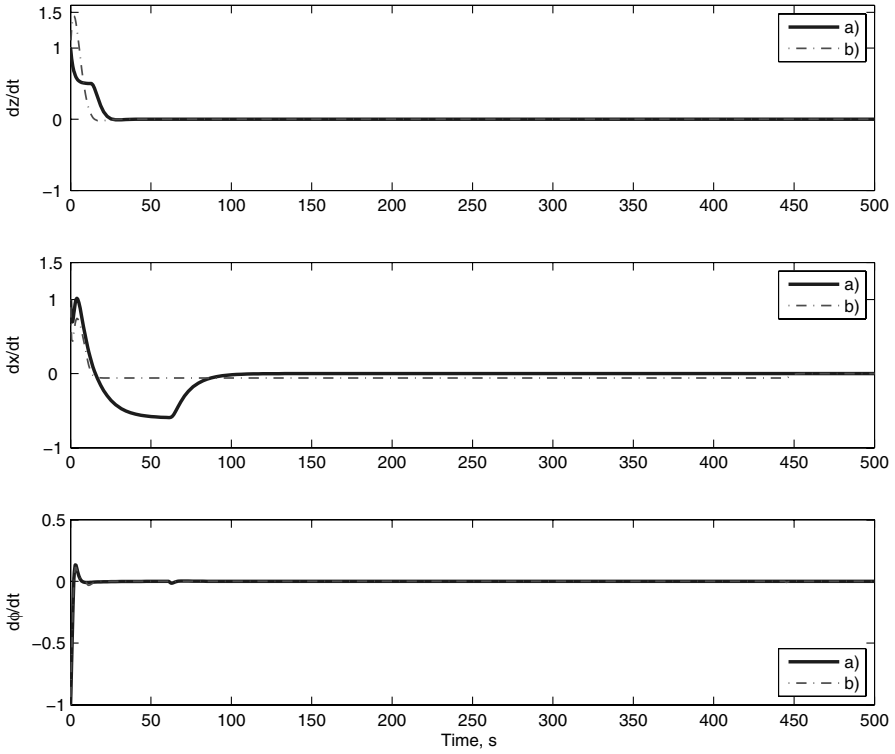

Fig. 5 States $\dot{z}$, $\dot{x}$ and $\dot{\phi}$ of the system: a) controllers (41) and (47), and b) controllers (48) and (49).

From Eq. (39), we have $z_1 \to 0$, from Eq. (37), $\xi_3 \to 0$. From Eq. (34), $z_2 \to 0$, from Eq. (32), $\xi_2 \to 0$. From Eq. (28), $z_3 \to 0$, from Eq. (26), $\xi_1 \to 0$, and from Eq. (22), $z_4 = x_4 \to 0$. Finally, from Eq. (24) $x_3 \to 0$, from Eq. (30) $x_2 \to 0$, and from Eq. (35) $x_1 \to 0$. Rewriting the control input u_2, we obtain

$$u = -\sigma_{b_4}(k_4 z_4) - \sigma_{b_3}(k_3 z_3) - \sigma_{b_2}(k_2 z_2) - \sigma_{b_1}(k_1 z_1) \tag{40}$$

IV. Simulation Results

In this section, we present the simulation results when applying the proposed controllers (7) and (40) to stabilize the PVTOL aircraft. Let us propose

$$u = \frac{f_1(z, \dot{z}) + mg}{\cos \sigma_{n_3}(\phi)} \tag{41}$$

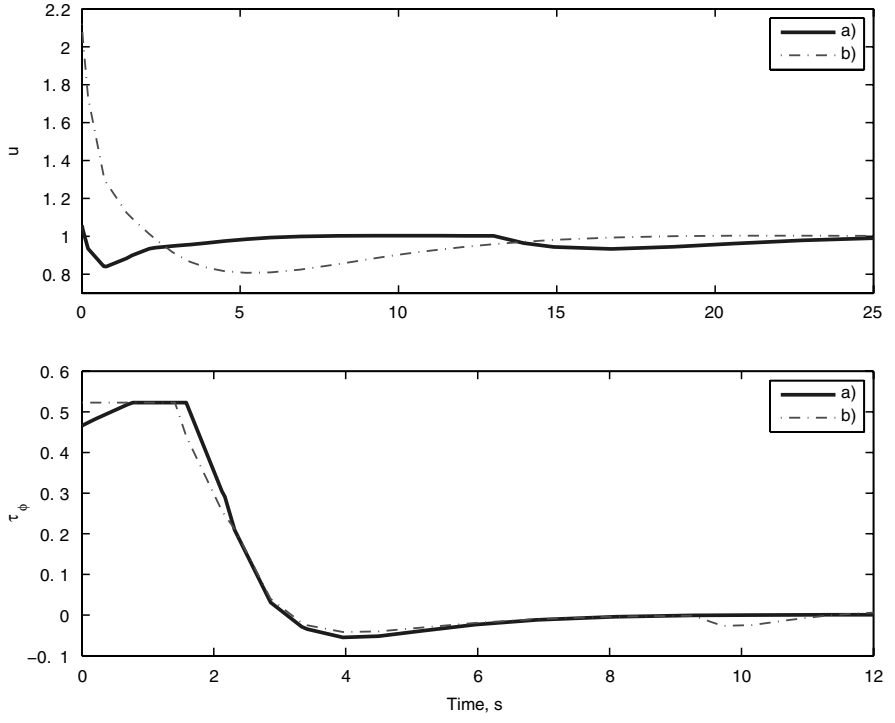

Fig. 6 A close-up view of control inputs u and τ_ϕ: a) controllers (41) and (47), and b) controllers (48) and (49).

Fig. 7 1-D helicopter.

where $f_1(z,\dot{z}) = -\sigma_{n_1}(a_1\dot{z}) - \sigma_{n_2}(a_2(z-z_d))$; $|\sigma_{n_i}(s)| \leq n_i$ $\forall\, i = 1, 2, 3$ is a saturation function; n_i, a_1, and a_2 are positive constant; and $n_3 < \pi/2$ and z_d is the constant desired altitude. Let us assume that, after a finite time T, $\phi(t)$ belongs to the interval $I_{\pi/2} = [(-\pi/2) + \bar{\epsilon}, (\pi/2) - \bar{\epsilon}]$ for some $\bar{\epsilon} > 0$ so that $\cos\sigma_{n_3}(\phi(t)) \neq 0$. Introducing Eq. (41) into Eq. (3) and normalizing $I = 1$, we obtain

$$m\ddot{z} = f_1(z,\dot{z}) \tag{42}$$

$$m\ddot{x} = -(f_1(z,\dot{z}) + mg)\tan\phi \tag{43}$$

$$\ddot{\phi} = \tau_\phi \tag{44}$$

Note that Eq. (42) represents two integrators in cascade. Note also from Sec. III.A that, for a time T_2 large enough, $f_1(z,\dot{z})$ is arbitrarily small and Eq. (43) reduces to $\ddot{x} = -g\tan\phi$. To further simplify the analysis, we will impose a very small upper bound on $|\phi|$ in such a way that the difference $\tan(\phi) - \phi$ is arbitrarily small. Therefore, the subsystem (43) and (44) reduces to

$$\ddot{x} = -g\phi \tag{45}$$

$$\ddot{\phi} = \tau_\phi \tag{46}$$

which represents four integrators in cascade. Making $\alpha, \gamma = 1$, and $\beta = -g$ and using Sec. III.B, we obtain

$$\tau_\phi = -\sigma_{b_4}(k_4 z_4) - \sigma_{b_3}(k_3 z_3) - \sigma_{b_2}(k_2 z_2) - \sigma_{b_1}(k_1 z_1) \tag{47}$$

with

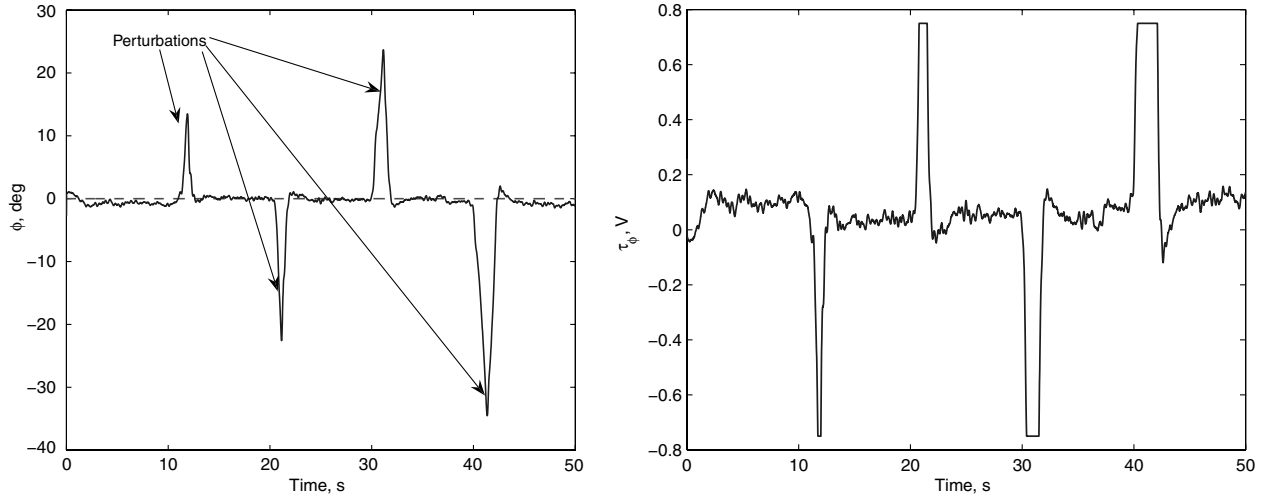

Fig. 8 ϕ angle and τ_ϕ control input. The dotted line represents the desired trajectory, in this case $\phi_d = 0$. The arrows indicate when the different perturbations are introduced. Note that the control input remains bounded.

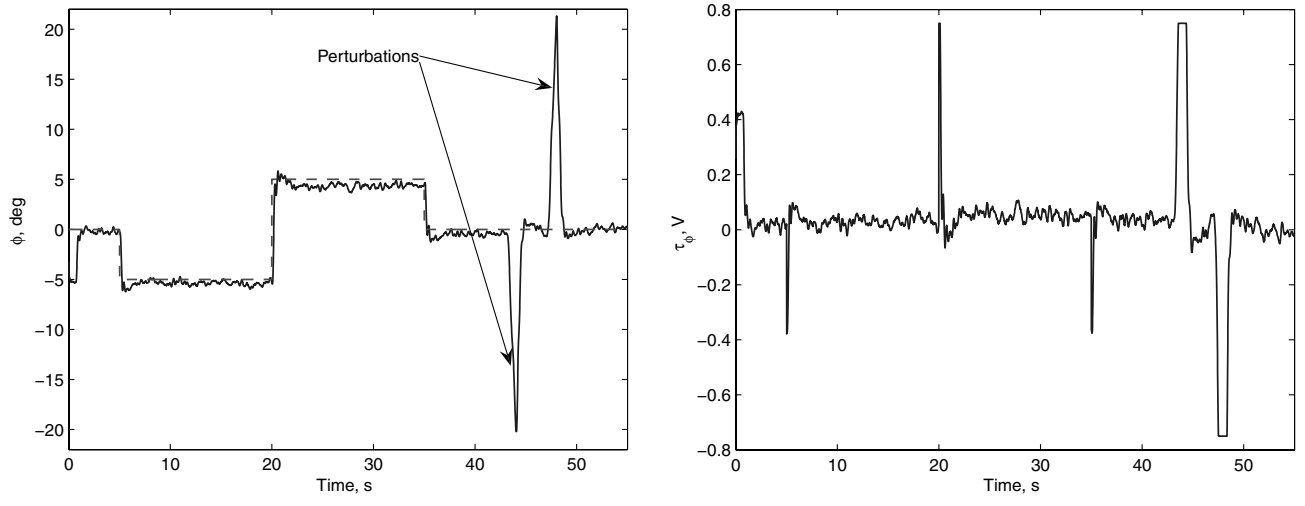

Fig. 9 ϕ angle and τ_ϕ control input. The dotted line represents the desired trajectory.

$$z_4 = \dot{\phi}, \qquad z_2 = z_3 + k_3\dot{\phi} - \frac{k_3k_4}{g}\dot{x}, \qquad z_3 = k_4\phi + \dot{\phi},$$
$$z_1 = z_2 + k_2\phi - \frac{k_2k_3k_4}{g}x - \frac{k_2(k_3+k_4)}{g}\dot{x}$$

The performance of the proposed control laws, Eqs. (41) and (47), is compared in simulation with respect to the controller proposed in Castillo et al. [1], that is,

$$\bar{u} = \frac{-\bar{a}_1\dot{z} - \bar{a}_2(z - z_d) + mg}{\cos\sigma_p(\phi)} \tag{48}$$

$$\bar{\tau}_\phi = -\sigma_a[\dot{\phi} + \sigma_b(\phi + \dot{\phi} + \sigma_c[2\phi + \dot{\phi} - \dot{x} + \sigma_d(3\phi + \dot{\phi} - 3\dot{x} - x)])] \tag{49}$$

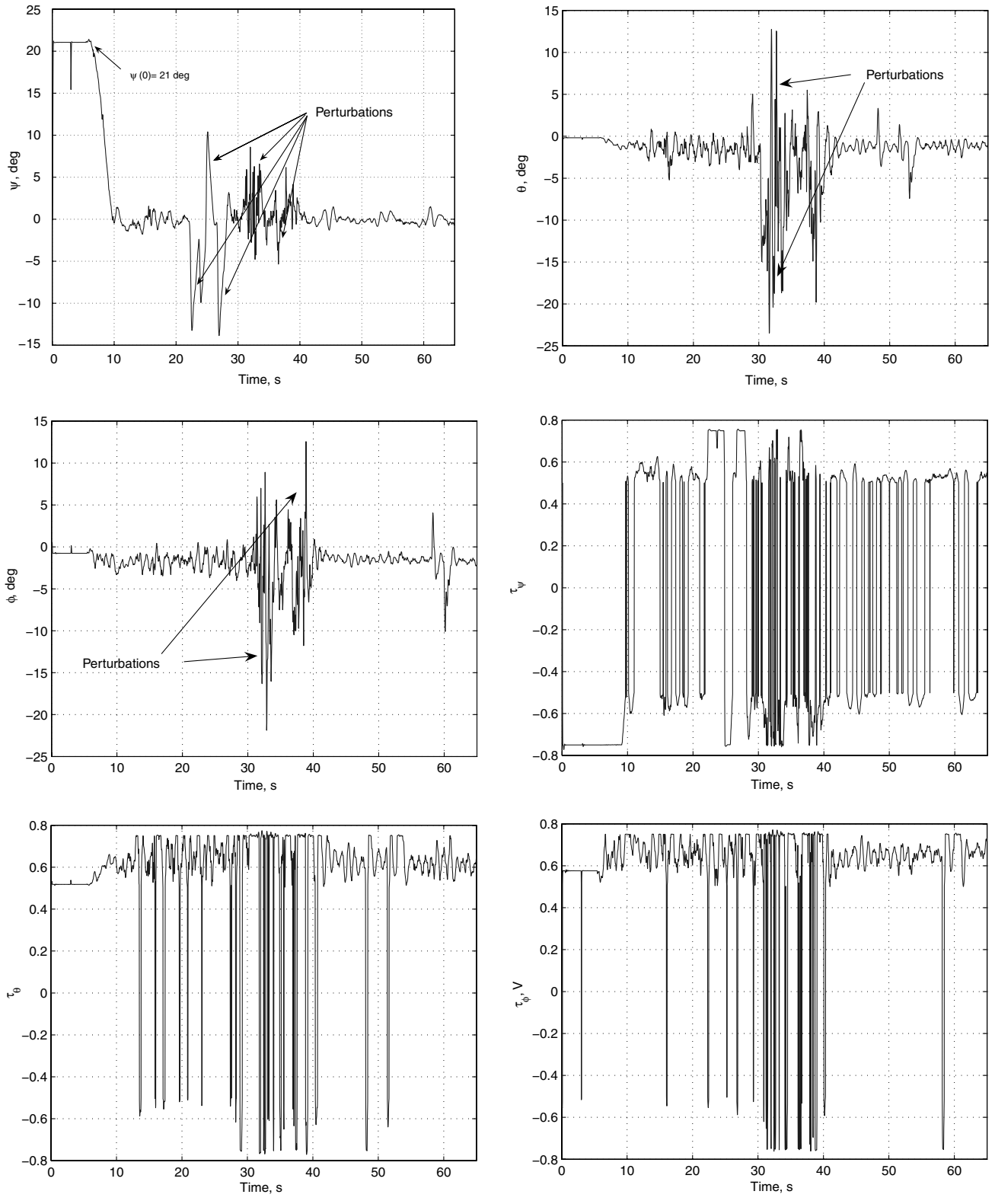

Fig. 10 Attitude stabilization of the quad-rotor rotorcraft and control inputs τ_ψ, τ_θ, and τ_ϕ.

Table 2 Gain values used to control the attitude of a VTOL aircraft

Control parameter	Value
$\bar{k}_1$	0.008
$\bar{k}_2$	0.5
b_1	0.25
b_2	0.5

where $\bar{a}_1$, $\bar{a}_2$, a, b, c, and d are positive constant and $0 < p < \pi/2$ (see [1] for more details). Note that the control input (49) is based on nested saturation functions.

We started the PVTOL aircraft at the position $(x(0), z(0), \phi(0)) = (20, 0, \pi/4)$ and $(\dot{x}(0), \dot{z}(0), \dot{\phi}(0)) = (1, 1, -1)$. The desired altitude is $z_d = 10$. The gain values used in this experiment are in Table 1.

Figure 4 shows the response of the closed-loop system to stabilize the PVTOL aircraft when applying the controller (41) and (47). In the same figure, we can observe the performance of the proposed controller with respect to the controller (48) and (49). Note from this figure that the convergence in the z position is faster with the control law in Castillo et al. [1]. This result is normal because that controller does not have saturation functions and has a linear performance. In the presence of perturbations, this controller is more sensible and the system dynamics could become unstable. Note also from Fig. 4 that the proposed controller performs better in the x position than the controller (48) and (49), and the convergence of the (x, ϕ) subsystem is faster even using the same upper bound in the control input τ_ϕ.

Figure 5 shows the linear and the angular velocities of the system. In this figure, there are no main features in either controller. The linear velocity $\dot{z}$ is not bounded when using the controller (48) but, when using the proposed controller (41), the performance of this state is better than the other one. Nevertheless, the other velocities ($\dot{x}$ and $\dot{\phi}$) remain bounded. Note from Fig. 5 that, when using the proposed controller, the convergence of $\dot{x}$ is faster than when using the controller in Castillo et al. [1]. Figure 6 (a close-up view) shows the performance of the control inputs (u and τ_ϕ). Note that the upper bound in the control input τ_ϕ is the same in both controllers, that is, $\tau_\phi \leq 0.523$, see Table 1. In Figs. 5 and 6, the solid lines represent the proposed controller and the dotted lines represent the controller in Castillo et al. [1].

V. Experimental Results

In this section, some experimental results are presented. We present these results in two parts. First, we test the performance of the controller (7) in a real-time experiment to stabilize the attitude of a VTOL aircraft and to reach a desired set point. Second, we stabilize the full model of the quad-rotor helicopter using the two proposed controllers.

A. Attitude Stabilization

We implement the controller (7) and (40) for the attitude stabilization of a VTOL aircraft. Note that the attitude dynamics of a VTOL aircraft can be represented by two integrators in cascade. We have validated the proposed controller in two helicopters: a 1-D helicopter and a 3-D free quad-rotor helicopter.

1. 1-D Helicopter

The 1-D helicopter consists of a decoupled quad-rotor helicopter mounted on a 1-DOF pivot joint such that the body can freely move only in the roll angle (see Fig. 7). The propellers generate a lift force that can be used to control the roll angle. The two propellers in the system are counter-rotating such that the yaw torque is practically zero.

The main objective of this section is to experimentally test the proposed controller for the regulation of the angular position. It is important to point out that a real helicopter cannot hover when the desired angular position is not close to zero.

The helicopter is attached on the y axis such that it can freely pivot around the x axis. We use an inertial measurement unit (IMU) sensor to measure the roll angular position (ϕ) and velocity ($\dot{\phi}$). Notice that the IMU sensor combines three angular rate gyros with three orthogonal dc accelerometers and three orthogonal magnetometers to output its orientation and angular rate. All of the controllers are implemented using a real-time XPC-Target toolbox from MATLAB®.

The goal is to stabilize the roll angle and experimentally test the robustness of the proposed controller. The angular dynamic of the roll angle is given by

$$\tau_\phi = \ddot{\phi} \tag{50}$$

From Eq. (7) and taking $\beta = 1$, we obtain

$$\tau_\phi = -\sigma_{b_2}(\bar{k}_2\phi_2) - \sigma_{b_1}(\bar{k}_1\phi_1) \tag{51}$$

The performance of the proposed controller when applied to stabilize the roll angle (ϕ) of a 1-D helicopter is shown in Fig. 8. We have manually perturbed the hovering vehicle. Note that the closed-loop system remains stable in the presence of aggressive perturbations. The parameters used are shown in Table 2.

The closed-loop system response when using a square wave as the desired trajectory is shown in Fig. 9. Two aggressive perturbations have been introduced to test the robustness of the controller. Note in this figure that the controller performs well.

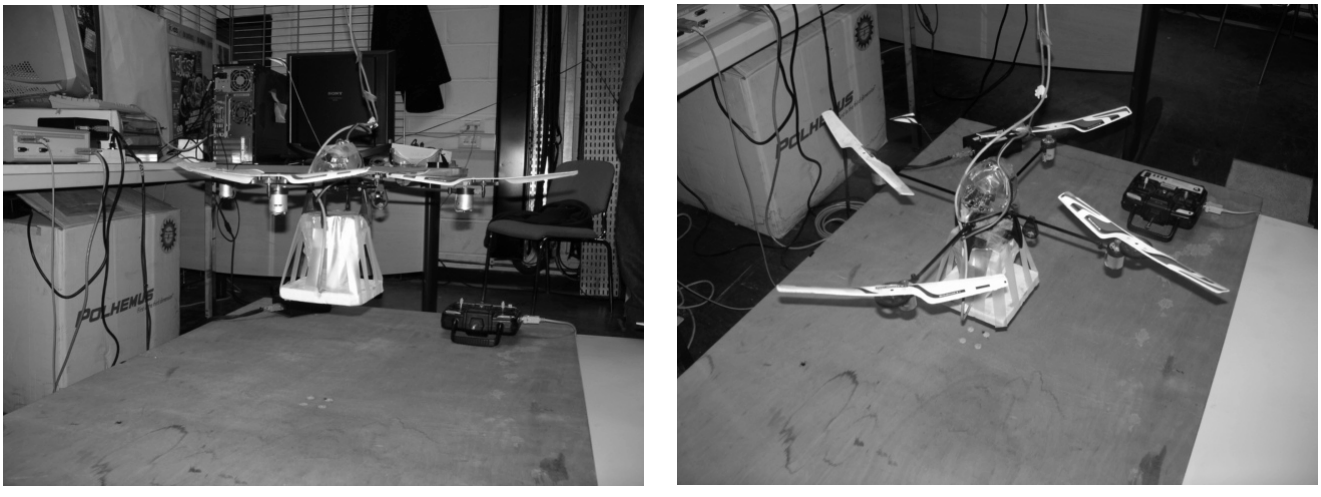

Fig. 11 Picture of the quad-rotor aircraft hovering.

2. Quad-Rotor Helicopter

The experimental platform is composed of a Draganflyer helicopter, a Futaba 72 MHz radio, a PC Pentium II, and a three-dimensional tracker system (POLHEMUS) for measuring the orientation (ψ, θ, ϕ) of the quad-rotor (for more details, see Castillo et al. [1]).

To apply the proposed control algorithm, (7), to the rotorcraft, the aircraft is placed in an arbitrary yaw angular position, which is

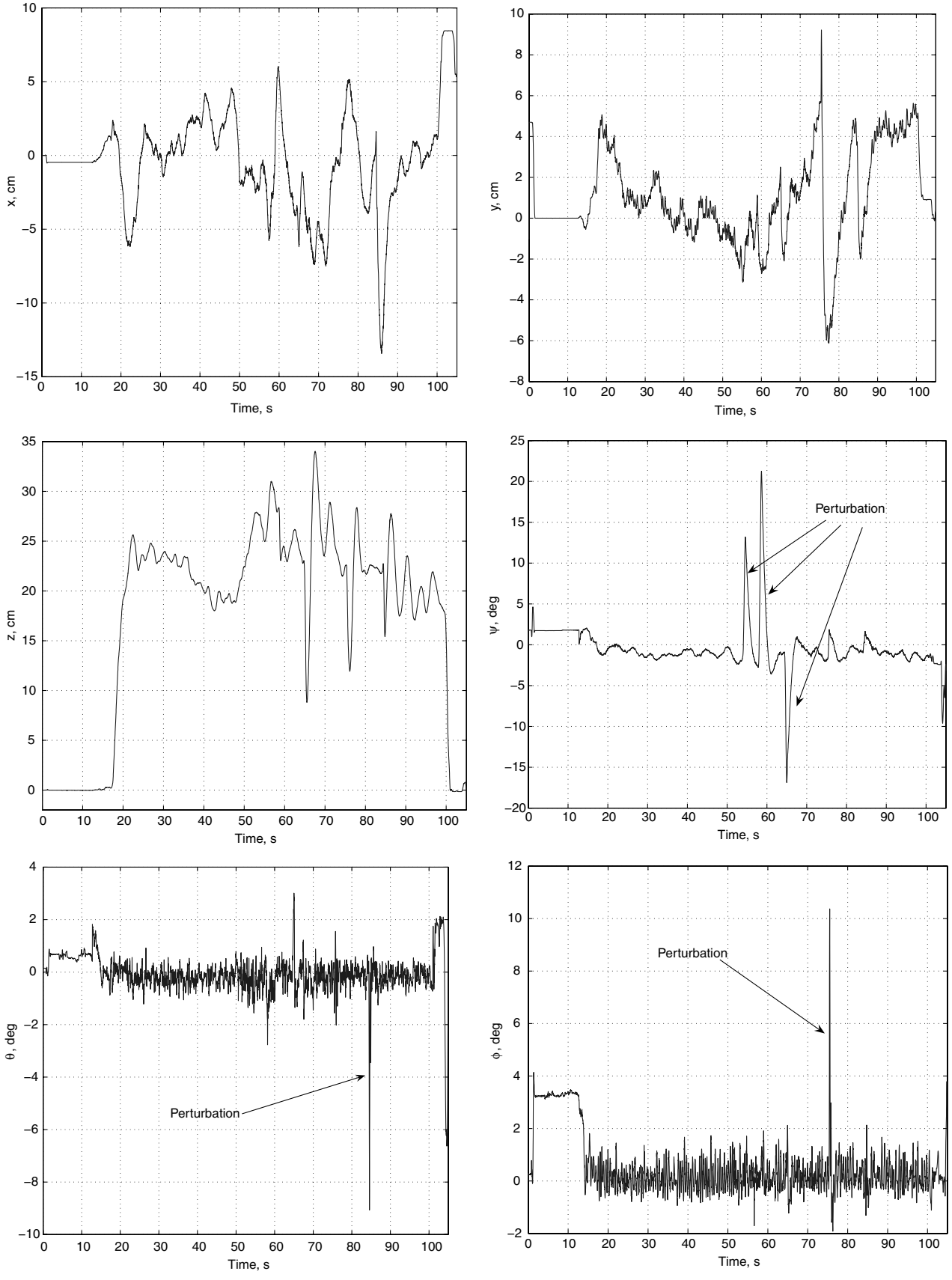

Fig. 12 Position and orientation of the aircraft.

$\psi = 21$ deg. The control objective is to make the rotorcraft hover while $(\psi, \theta, \phi) = (0, 0, 0)$. Figure 10 shows the performance when applying the proposed controller (7) to stabilize the attitude of a free quad-rotor helicopter. For this experiment $\beta, k = 1$; in addition, the parameters used are shown in Table 2.

The system response to aggressive perturbations in the angular displacement has been also analyzed. In this experiment, we have perturbed the orientation of the helicopter, that is, we reached out and pushed on the hovering vehicle with our hands. The yaw, pitch, and roll angles were perturbed from ± 10 to ± 25 deg. As shown in Fig. 10, the response remains bounded. Also, it should be noted in Fig. 10 that the control inputs are bounded.

B. Stabilization of Quad-Rotor Aircraft

In this section, we present the real-time experimental results obtained when applying the proposed control strategies to a quad-rotor aircraft. The nonlinear control algorithm will be obtained for the linear model of the helicopter. We show in this section that the proposed controllers perform well in practice.

Linearizing Eq. (5), we obtain

$$\ddot{x} = g\theta, \qquad \ddot{\psi} = u_2, \qquad \ddot{y} = -g\phi, \qquad \ddot{\theta} = u_3, \qquad \ddot{z} = u_1, \qquad \ddot{\phi} = u_4$$

where $(x_1 \;\; x_2 \;\; x_3 \;\; x_4 \;\; x_5 \;\; x_6 \;\; x_7 \;\; x_8 \;\; x_9 \;\; x_{10} \;\; x_{11} \;\; x_{12})^T = (x \;\; \dot{x} \;\; y \;\; \dot{y} \;\; z \;\; \dot{z} \;\; \psi \;\; \dot{\psi} \;\; \theta \;\; \dot{\theta} \;\; \phi \;\; \dot{\phi})^T$ and $(u_1 \; u_2 \; u_3 \; u_4)^T = (u - g \;\; \tau_\psi \;\; \tau_\theta \;\; \tau_\phi)$.

To stabilize the altitude z and the yaw angle ψ, we use the controller (7), and then we obtain

$$u_1 = -\sigma_{b_{z_2}}(\bar{k}_{z_2}\dot{z}) - \sigma_{b_{z_1}}(\bar{k}_{z_1}(z - z_d)) \tag{52}$$

$$u_2 = -\sigma_{b_{\psi_2}}(\bar{k}_{\psi_2}\dot{\psi}) - \sigma_{b_{\psi_1}}(\bar{k}_{\psi_1}(\psi - \psi_d)) \tag{53}$$

where $\beta = 1$ and $k = 1$. To stabilize the (x, θ) and (y, ϕ) subsystems, we use the controller (40). Thus, we obtain

$$u_3 = -\sigma_{b_4}(k_4 z_4) - \sigma_{b_3}(k_3 z_3) - \sigma_{b_2}(k_2 z_2) - \sigma_{b_1}(k_1 z_1) \tag{54}$$

with

$$\alpha, \gamma = 1, \qquad z_3 = k_4\theta + \dot{\theta}, \qquad \beta = g,$$
$$z_2 = z_3 + k_3\dot{\theta} - \frac{k_3 k_4}{g}\dot{x}, \qquad z_4 = \dot{\theta},$$
$$z_1 = z_2 + k_2\theta - \frac{k_2 k_3 k_4}{g}x - \frac{k_2(k_3 + k_4)}{g}\dot{x}$$

and

$$u_4 = -\sigma_{b_4}(k_4 z_4) - \sigma_{b_3}(k_3 z_3) - \sigma_{b_2}(k_2 z_2) - \sigma_{b_1}(k_1 z_1) \tag{55}$$

with

$$\alpha, \gamma = 1, \qquad z_3 = k_4\phi + \dot{\phi}, \qquad \beta = -g,$$
$$z_2 = z_3 + k_3\dot{\phi} + \frac{k_3 k_4}{g}\dot{y}, \qquad z_4 = \dot{\phi},$$
$$z_1 = z_2 + k_2\phi + \frac{k_2 k_3 k_4}{g}y + \frac{k_2(k_3 + k_4)}{g}\dot{y}$$

Figure 11 shows two photos of the quad-rotor aircraft in hover. Figure 12 shows the performance of the helicopter when applying the proposed controller. Note that the control objective is to reach the position $(x, y, z) = (0, 0, 20)$ in centimeters while $(\psi, \theta, \phi) = (0, 0, 0)$ deg. To improve the performance of the experiment, we have experimentally tuned the parameters in the saturation functions. Table 2 shows the parameters that we have used. We have perturbed the angles of the aircraft. Figure 13 presents the control inputs obtained in this experiment.

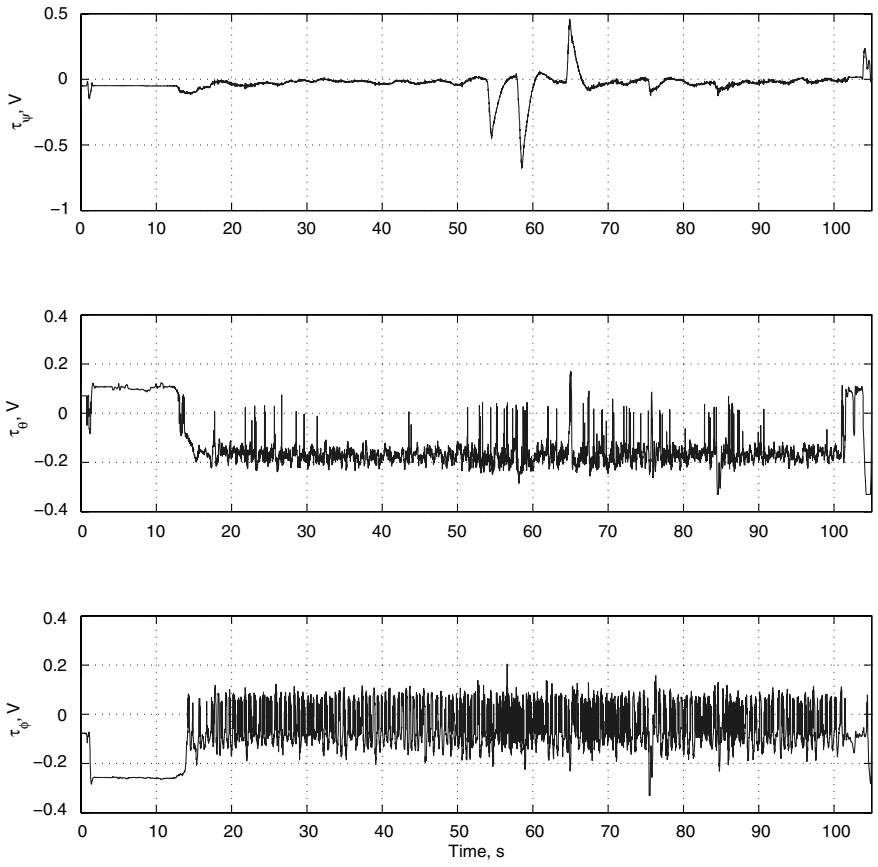

Fig. 13 Control inputs τ_ψ, τ_θ, and τ_ϕ.

VI. Conclusions

In this paper, a simple real-time stabilization of a VTOL aircraft has been presented. The control strategy was obtained using saturation functions and the Lyapunov analysis. The proposed controller was tested in simulation and in real-time experiments in two prototypes of quad-rotor helicopters. The experimental results show that the controller performs well even in presence of aggressive perturbations.**

References

[1] Castillo, P., Lozano, R., and Dzul, A., *Modelling and Control of Mini-Flying Machines*, Advances in Industrial Control, Springer–Verlag, Berlin/New York/Heidelberg, July 2005, ISBN 1-85233-957-8.

[2] McCormick, B. W., *Aerodynamics Aeronautics and Flight Mechanics*, Wiley, New York, 1995.

[3] Etkin, B., and Reid, L. D., *Dynamics of Flight*, Wiley, New York, 1959, ISBN 0-471-03418-5.

[4] Hauser, J., Sastry, S., and Meyer, G., "Nonlinear Control Design for Slightly Nonminimum Phase Systems: Application to V/STOL Aircraft," *Automatica*, Vol. 28, No. 4, 1992, pp. 665–679. doi:10.1016/0005-1098(92)90029-F

[5] Marconi, L., Isidori, A., and Serrani, A., "Autonomous Vertical Landing on an Oscillating Platform: An Internal-Model Based Approach," *Automatica*, Vol. 38, No. 1, Jan. 2002, pp. 21–32. doi:10.1016/S0005-1098(01)00184-4

[6] Wen, J. T-Y., and Kreutz-Delgado, K., "The Attitude Control Problem," *IEEE Transactions on Automatic Control*, Vol. 36, No. 10, 1991, pp. 1148–1162. doi:10.1109/9.90228

[7] Wie, B., Weiss, H., and Arapostathis, A., "Quaternion Feedback Regulator for Spacecraft Eigenaxis Rotations," *Journal of Guidance, Control, and Dynamics*, Vol. 12, No. 3, 1989, pp. 375–380.

[8] Ickes, B. P., "A New Method for Performing Digital Control System Attitude Computations Using Quaternions," *AIAA Journal*, Vol. 8, No. 1, 1970, pp. 13–17.

[9] Kane, T. R., "Solution of Kinematical Differential Equations for a Rigid Body," *Journal of Applied Mechanics*, Vol. 40, No. 1, 1973, pp. 109–113.

[10] Lozano, R., Brogliato, B., Egeland, O., and Maschke, B., *Passivity-Based Control System Analysis and Design*, Communications and Control Engineering Series, Springer–Verlag, 2000.

[11] Fantoni, I., and Lozano, R., *Control of Nonlinear Mechanical Underactuated Systems*, Communications and Control Engineering Series, Springer–Verlag, Berlin/New York/Heidelberg, 2001.

[12] Olfati-Saber, R., "Global Configuration Stabilization for the VTOL Aircraft with Strong Input Coupling," *Proceedings of the 39th IEEE Conf. on Decision and Control*, Vol. 4, Inst. of Electrical and Electronics Engineers, Piscataway, NJ, 2000, pp. 3588–3589.

**Data available online at http://www.hds.utc.fr/~asanchez [retrieved 30 April 2008].